Supporting Information

Fabrication and characterization of the high surface area MoS_2@WS_2 heterojunction for ultra-sensitive NO_2 detection at room temperature

Muhammad Ikram[a], Lujia Liu[a], Yang Liu[a], Laifeng Ma[a], He Lv[a], Mohib ullah[a], Lang He[a], Hongyuan Wu[b], Ruihong Wang[*a], Keying Shi[*a]

[a] *Key Laboratory of Functional Inorganic Material Chemistry, Ministry of Education. School of Chemistry and Material Science, Heilongjiang University, Harbin, 150080, P. R. China.*

[b] *College of Chemistry and Chemical Engineering, Qiqihar University, Qiqihar 161006, P. R. China.*

*Corresponding author: Tel.: +86 451 86609141; +86 451 86604920

E-mail: 2003wangruihong@163.com, shikeying2008@163.com

Abstract: Supporting information provide shows; (i) gas delivery system setup, (ii) EDS spectrum of MWS-1, and MWS-3, (iii) TEM, HRTEM and SEAD pattern of the MWS-1 nanocomposite, (iv) TEM, HRTEM, STEM and mapping images of the MWS-2, (v) TEM, HRTEM and SEAD pattern of the MWS-3, (vi, (vii) TEM, HRTEM, SEM and AFM images of the pristine expanded/exfoliated MoS_2 NSs, (viii) XRD pattern of the bulk MoS_2 NSs and WS_2, the comparative peak (002) intensities of the bulk MoS_2 with exfoliated MoS_2 NSs, (ix) Fitted impedance parameters all of the samples, (x) MS plots of all the sensor samples, (xi), (xii) XPS spectra of the pristine MoS_2 and the peak position of the pristine MoS_2, MWS-2 and of the used MWS-2 nanocomposite, (xiii) Dynamical response transient of the pristine MoS_2 NSs, MWS-1, and of the MWS-3 nanocomposites, (xiv) table of the comparative response and response/recovery time all of the samples, (xv) UV-vis spectra, Scheme of kelvin probe, and the contact diagram of the MoS_2 and WS_2 before and after contact.

Table of contents

S12 **Table S2, Fig. S10:** XPS peak position of the pristine MoS_2 NSs, and of the fresh and used MWS-2 nanocomposites, to show the shifting of peak positions. Response-recovery curve to different NO_2 concentration at RT in air.

S13 **Fig. S11 Table S3:** The effect of humidity. Response, response/recovery time all of the sensors to NO_2 gas at RT.

S14 **Fig S12, Fig S13:** Uv-vis spectra of pristine MoS_2 and WS_2 nanosheets and Scheme of Kelvin probe test.

S15 **Scheme S2:** Band diagram of MoS_2 and WS_2 before and after contact.

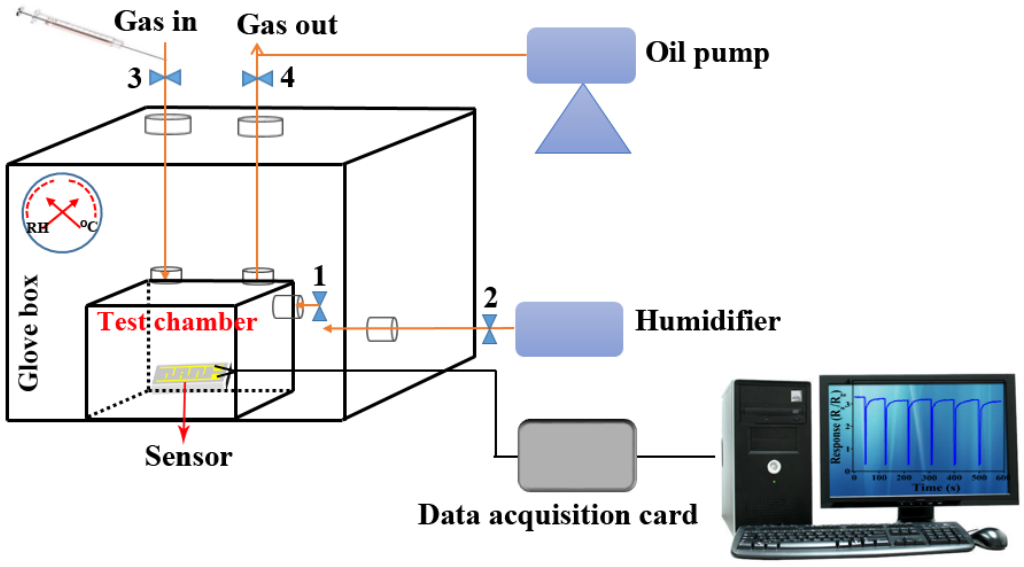

Scheme S1. The gas delivery system diagram for the sensing process.

The schematic diagram of the gas sensing delivery system presented in scheme S1. In the first step, the modified Au interdigitated electrode installed to the test chamber of the system, and connected with external environment through valve 2 and 4. At this time the valve 1 kept open, and the chamber was flush by fresh air to remove all of the impurities from test chamber and from homemade glove box. In next step, the valve 3 and 4 become close, and the system (test

chamber and homemade glove box) humidified with the help of valve 2 to achieved the desired humidity. The humidity of the system were monitored by humidity meter. After short time, the glove box and testing chamber achieved the same humidity, and then close valve 1. Finally, the valve 3 was open to inject the target gas to test chamber. When the resistance become balance, the valve 4 was open and the purging with fresh air with the help of oil pump till to achieved the resistance of the sensor to the initial state. This was finish one cycle of the response-recovery. The former three stages were repeated and the second response–recovery cycle was complete. In addition, the concentration of the target gas were control by using micro-syringe, and the repetition were conducted by using five sensors under each sensor detection.

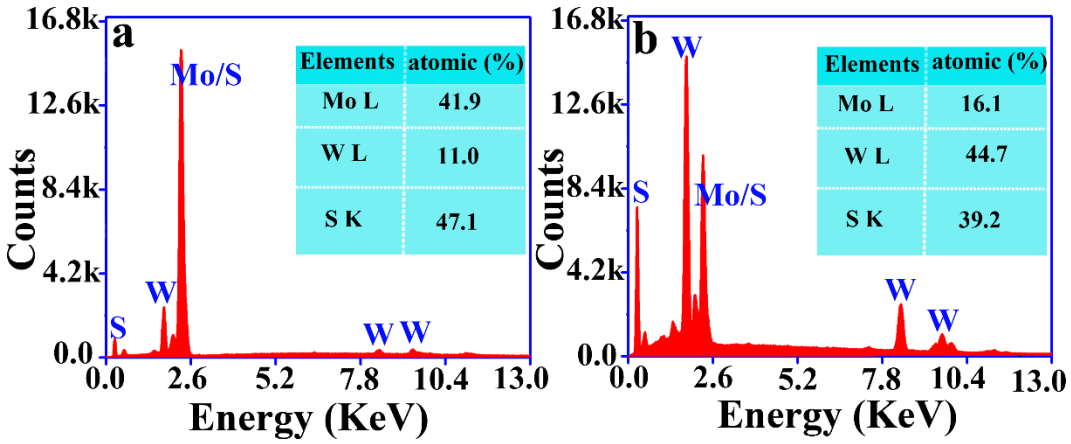

Fig. S1 (a, b) EDS spectrum of the MWS-1, and MWS-3 nanocomposite.

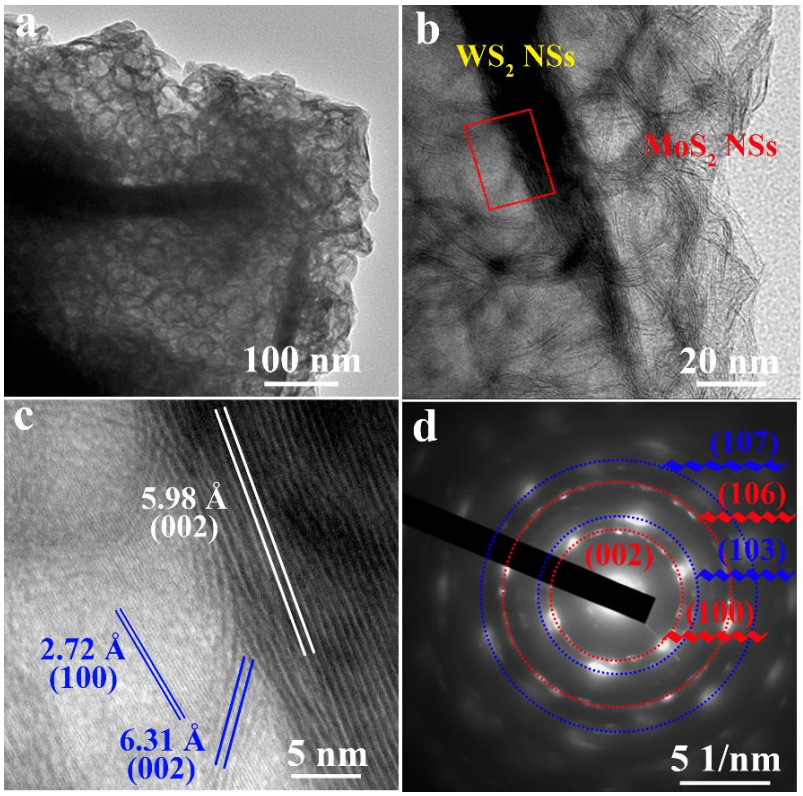

Fig. S2 (a, b) TEM images, (c) HRTEM image (white lines show WS_2, blue lines indicate MoS_2), (d) SAED pattern of MWS-1 nanocomposite (the ring marked as blue and red dash lines express the hexagonal structure of WS_2 and MoS_2 NSs, respectively).

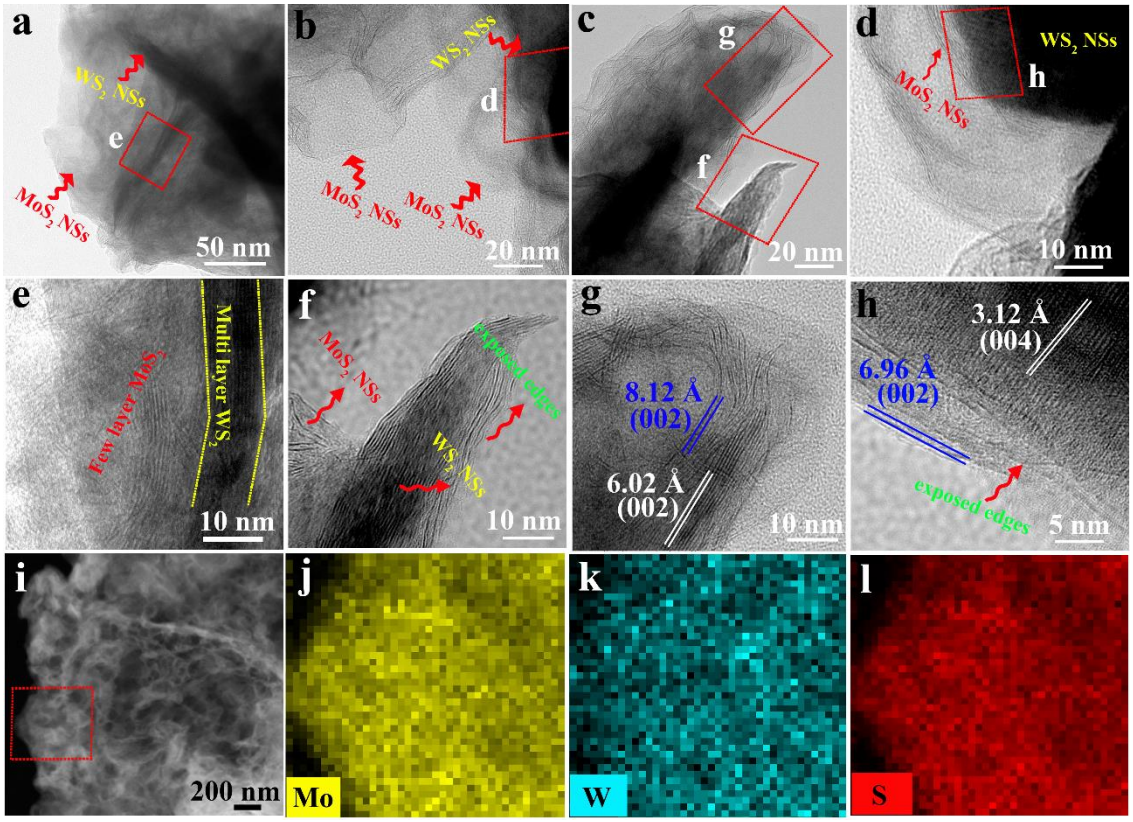

Fig. S3 (a-c) TEM images, (d-h) HRTEM images, (i) STEM image, and (j-l) Element mapping of the corresponding STEM image of THE MWS-2 nanocomposite (white lines show WS_2, blue lines indicate MoS_2).

The bright field STEM image and corresponding element mapping more confirm the spatial homogeneous distribution of Mo, S, and W elements in MWS-2 nanocomposite, and also revealed the high compactible morphology of MoS_2 and WS_2 NSs in MWS-2 (Figure S3 (i-l)).

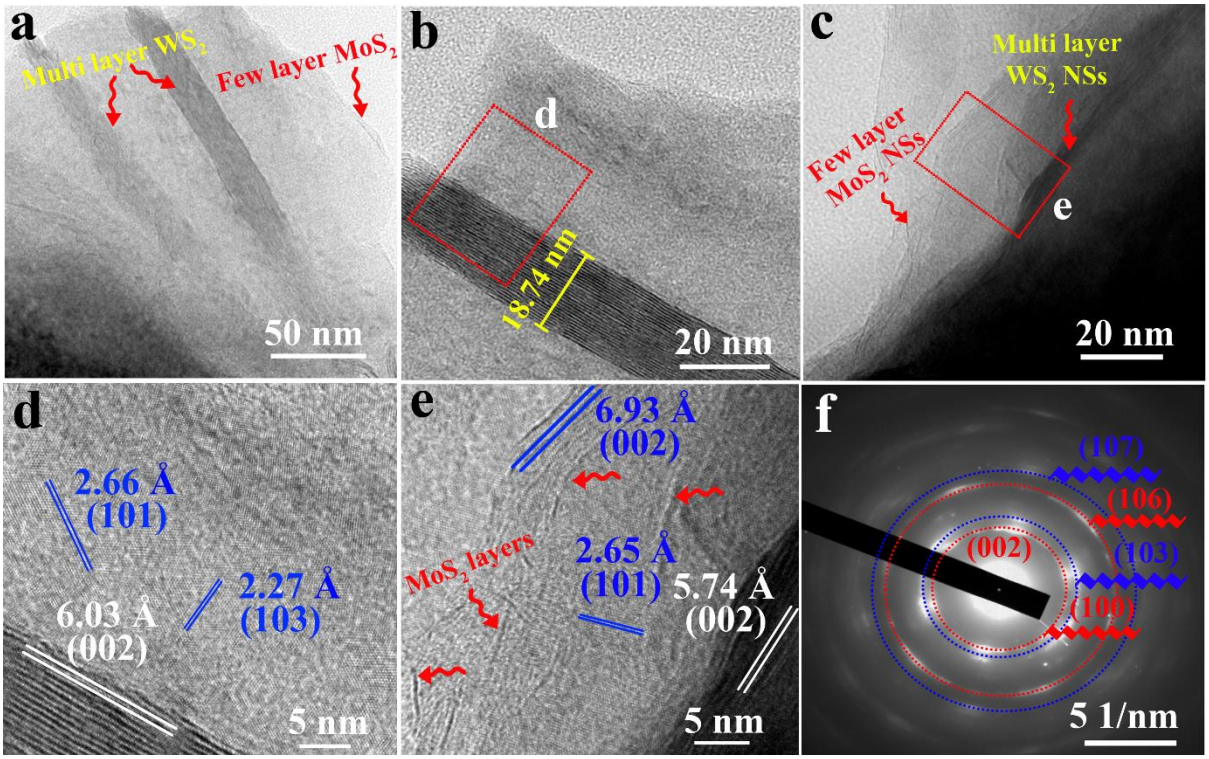

Fig. S4 (a-c) TEM images, (d, e) HRTEM images (white lines show WS_2, blue lines indicate MoS_2), (f) SAED pattern of the MWS-3 nanocomposite (the ring marked as blue and red dash lines express the hexagonal structure of WS_2 and MoS_2 NSs, respectively).

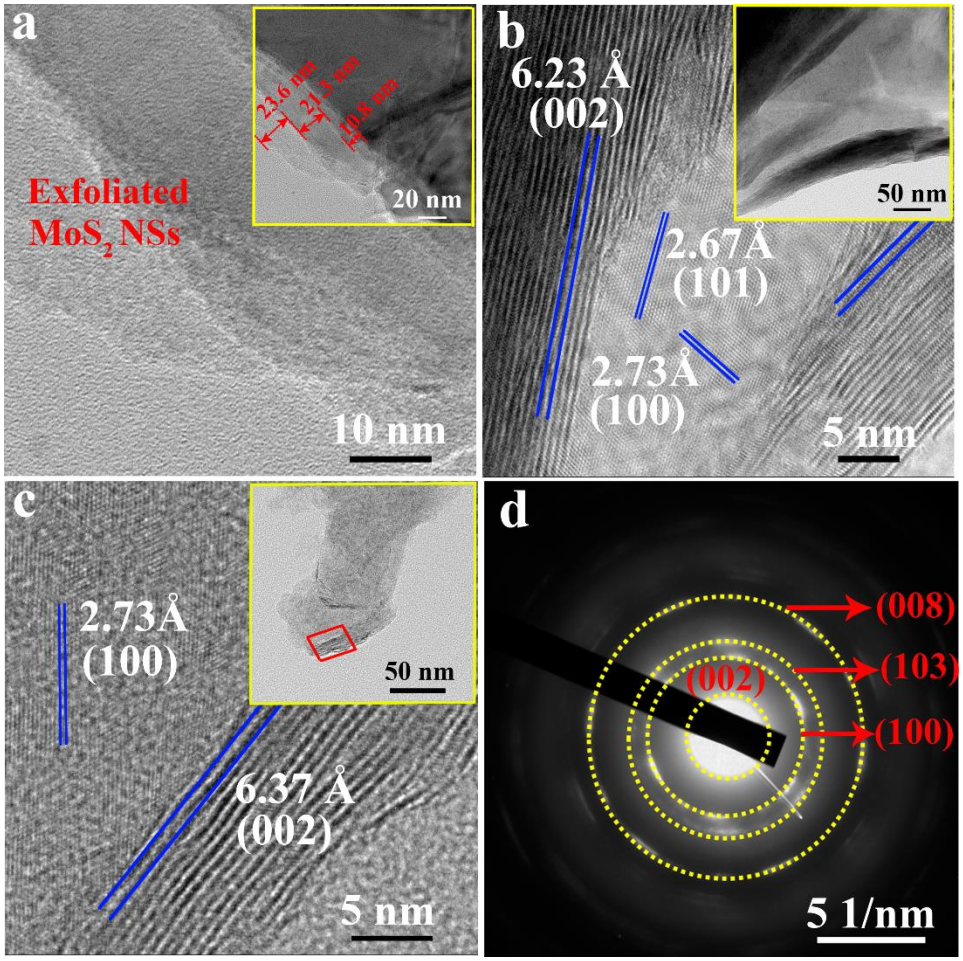

Fig. S5 (a, b) HRTEM images and the inset of TEM images, (d) SAED pattern of the pure expanded/exfoliated MoS_2 NSs.

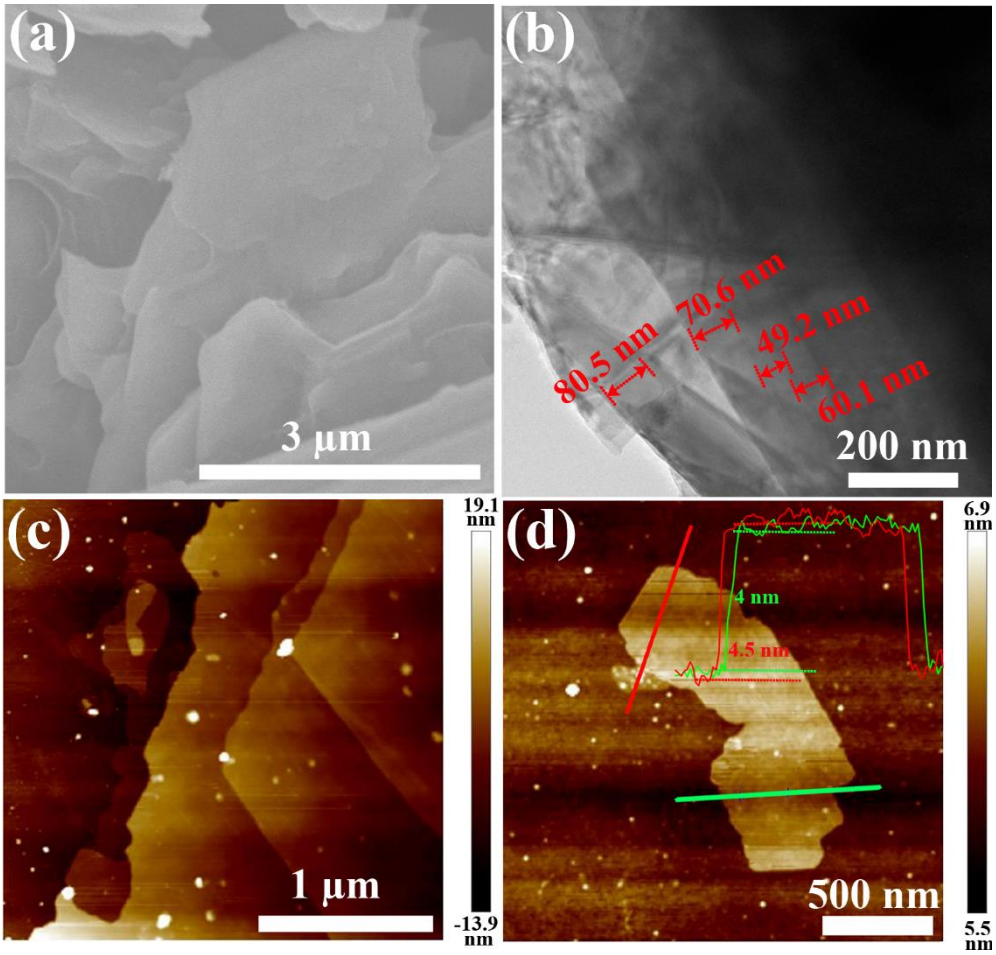

Fig. S6 Representation of the highly expanded/exfoliated pristine MoS_2 NSs, (a) SEM image, (b) TEM image, (c, d) AFM images with height profile (inset).

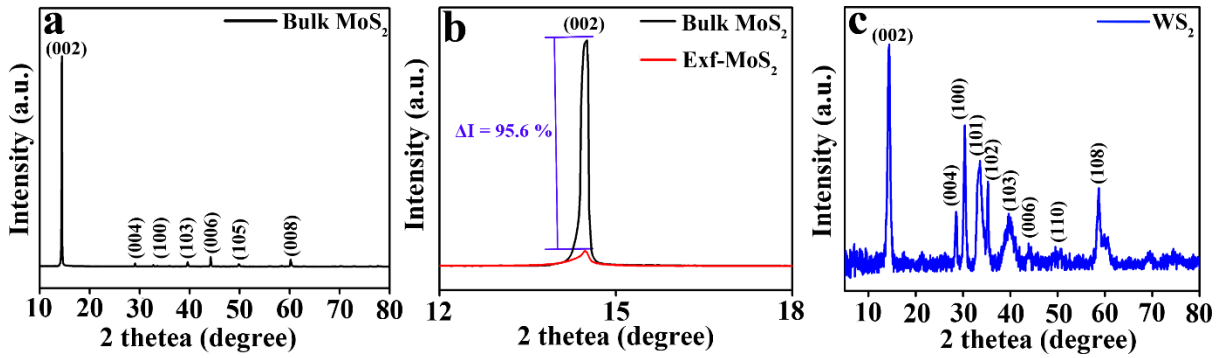

Fig. S7 (a) XRD spectra of bulk MoS_2 NSs; (b) Comparative peak of bulk MoS_2 with exfoliated MoS_2 NSs (ΔI = change in intensity); (c) XRD spectra of WS_2.

Table S1. Fitted impedance parameters of samples.

Samples	Pristine exfoliated MoS_2 NSs	MWS-1	MWS-2	MWS-3
R_{Ω} (Ω)	1017.5	629.1	**487.5**	564.8
R_{ct} (Ω)	9306	5518	**3975**	4504

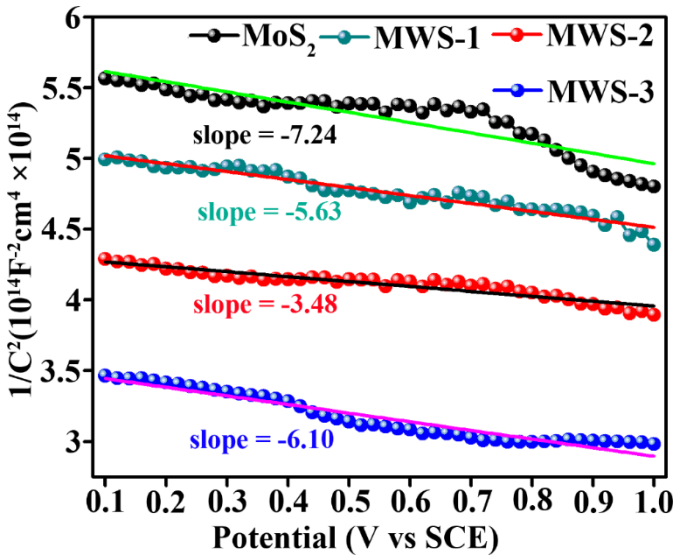

Fig. S8 The comparative MS plots of the pristine MoS_2 NSs with all of the composites (Measurement in the solution of 5 mM $Fe(CN)_6^{3-/4-}$ containing 0.1 M KCl).

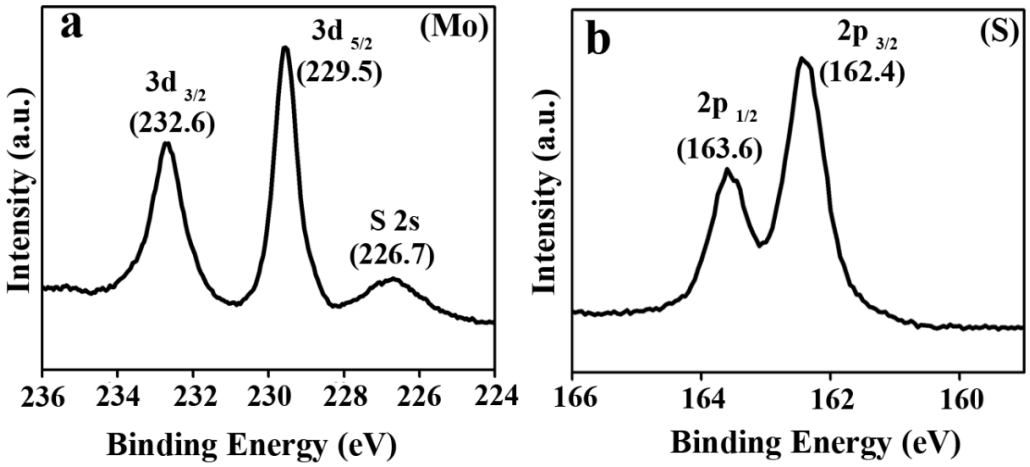

Fig. S9 (a, b) The XPS spectra of Mo 3d and S 2p of the pure expanded/exfoliated MoS_2 NSs.

Table S2. The comparative XPS peaks position of the pure MoS_2 NSs, fresh MWS-2 and of the used MWS-2 nanocomposite.

	Binding energy (eV)			
Samples	(Mo) $3d_{5/2}$ / $3d_{3/2}$	(S) $2p_{3/2}$ / $2p_{1/2}$	(W) $4f_{7/2}$ / $4f_{5/2}$	(N) 1s
Pure MoS_2	229.5/232.6	162.4/163.6	------	------
MWS-2 (Fresh)	228.5/231.7	162.2/161.2	31.8/35.2	------
MWS-2 (Used)	229.0/232.5	162.5/161.4	32.0/35.4	406.3/402.9

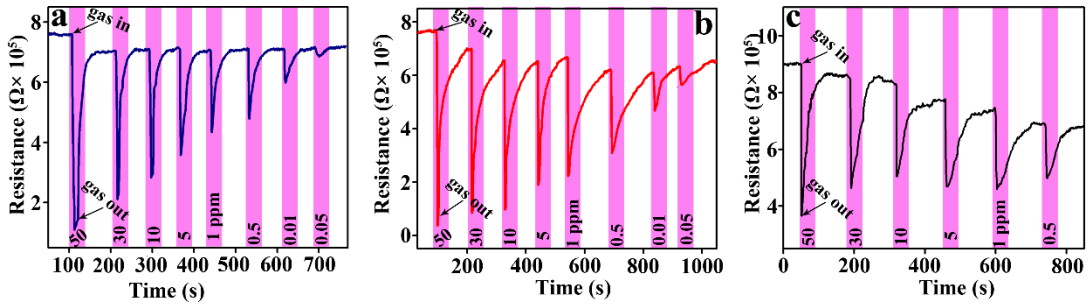

Fig. S10 Dynamical response transient of (a) MWS-1, (b) MWS-3, (c) exfoliated MoS_2 NSs to NO_2 gas at room temperature.

The detailed results specified that pure MoS_2 NSs shows poor response to NO_2 gas at different concentration with sluggish response/recovery time. While in the nanocomposites, MWS-2 shows excellent gas sensing performance compare to MWS-1, and MWS-3 sensors, which might be due to the good morphology, high surface area and appropriate concentration of MoS_2 and WS_2.

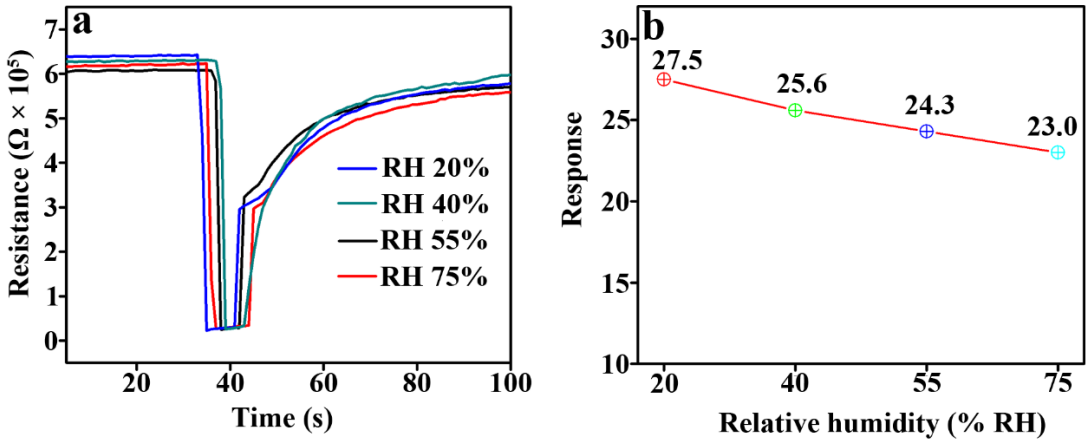

Fig. S11 (a) Response-recovery curves of the MWS-2 to 50 ppm NO_2 gas in different relative humidity at RT; (b) the gas sensor response corresponding to Figure (a).

Table S3. Response, response time and recovery time of the sensors to NO_2 at room temperature in 25 – 30 % humidity.

Sensors	**MoS_2**			**MWS-1**			**MWS-2**			**MWS-3**		
NO_2 (ppm)	**Response**	**t_{res}**	**t_{rec}**	**Response**	**t_{res}**	**t_{rec}**	**Response**	**t_{res}**	**t_{rec}**	**Response**	**t_{res}**	**t_{rec}**
50	2.47	5.8	54.9	7.01	3.4	35.7	**26.12**	**1.6**	**27.7**	20.88	1.9	53.3
30	1.84	6.9	52.2	3.33	4.0	30.4	**14.09**	**1.9**	**24.0**	8.31	2.7	56.5
10	1.63	8.5	53.8	2.49	4.4	31.4	**10.23**	**2.1**	**23.4**	6.76	3.1	52.8
5	2.03	9.2	51.2	2.0	4.9	29.3	**8.95**	**2.8**	**22.5**	3.46	4.0	46.9
1	1.62	10.3	56.2	1.65	5.6	30.4	**3.82**	**3.4**	**20.0**	3.01	3.9	50.8
0.5	1.35	10.8	48.5	1.48	6.0	32.0	**2.05**	**4.2**	**20.6**	1.98	5.1	49.1
0.1				1.18	6.5	26.6	**1.35**	**4.7**	**19.4**	1.29	5.8	40.0
0.05				1.04	7.2	18.6	**1.19**	**5.3**	**18.1**	1.1	6.1	37.8
0.01							**1.14**	**6.0**	**16.0**			

t_{res} = Response Time (s), t_{rec} = Recovery Time (s)

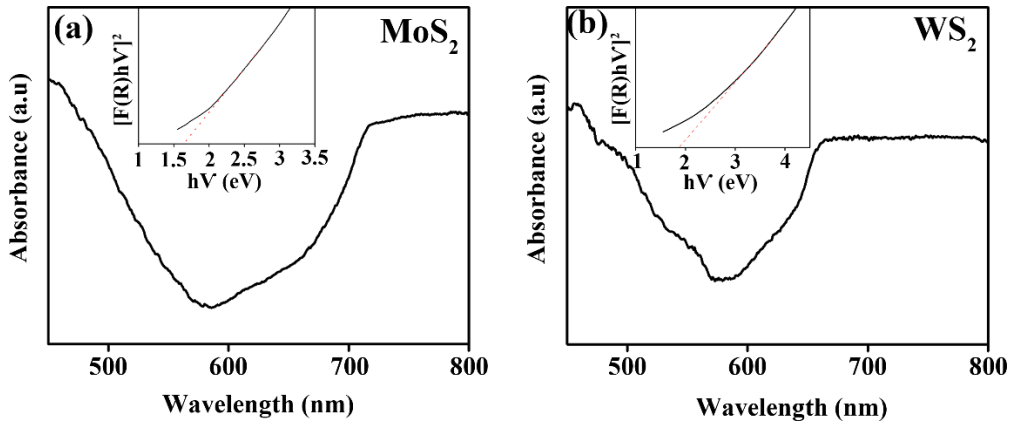

Fig. S12 (a, b) UV-vis diffused reflectance spectra of pristine MoS_2 and WS_2 nanosheets; inset is the corresponding plots of transformed Kubelka-Munk verses the energy light.

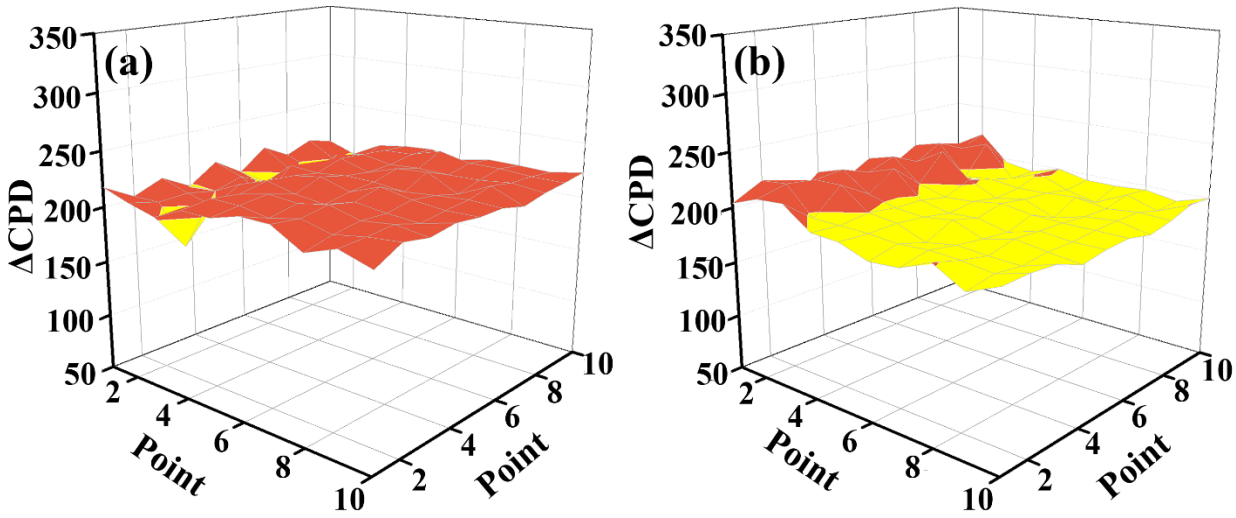

Fig. S13 Scheme of Kelvin probe of (a) MoS_2, (b) WS_2

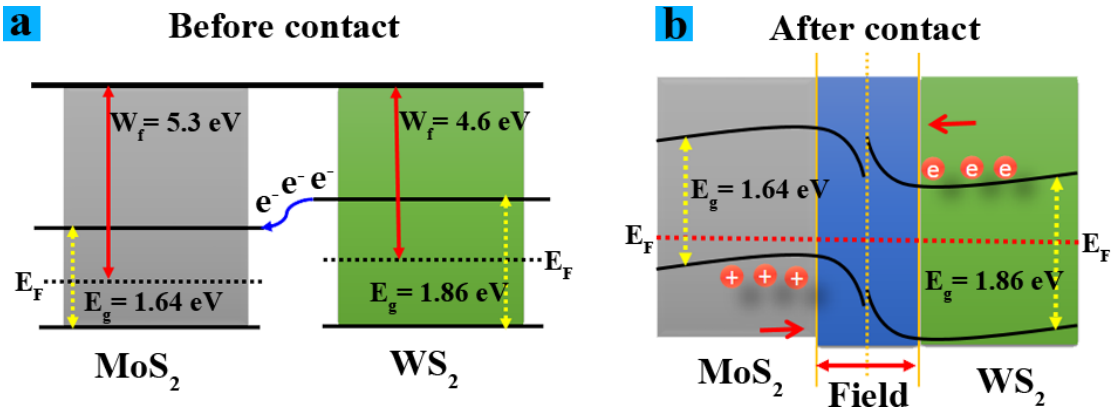

Scheme S2. Band diagram of the MoS_2@WS_2 heterojunction before and after contact.